*Vedran Carević[1], Mihael Bučko[2], Ivan Ignjatović[1], Jelena Bajat[3,]**

*[1]University of Belgrade, Faculty of Civil Engineering, Department of Materials and Structures, Belgrade; [2]University of Defense, Military Academy, Belgrade; [3]University of Belgrade, Faculty of Technology and Metallurgy, Department of Physical Chemistry and Electrochemistry, Belgrade*

Scientific paper
ISSN 0351-9465, E-ISSN 2466-2585
https://doi.org/10.62638/ZasMat2004



Zastita Materijala 67 ()
(2026)

# The influence of cracks on the salt scaling resistance and chloride ingress in recycled aggregate concrete**

## ABSTRACT

*Recycled concrete aggregate (RAC) offers a promising solution to reduce raw material use, energy consumption, and waste. However, its durability remains a concern. Due to low tensile strength, cracking under load is likely, which can impact concrete's longevity. In this paper the influence of loading induced cracks (0.08 mm and 0.20 mm) on RAC resistance to salt scaling and the impact of previous carbonation on their resistance to salt scaling was presented. The influence of cracks on the development of reinforcement corrosion on long probe as well as corrosion mapping in relation to the position of the crack was analyzed. The onset and the development of corrosion process on steel reinforcing probes were monitored by three different electrochemical techniques: open circuit potential monitoring, electrochemical impedance spectroscopy and linear polarization resistance. It was shown that the presence of cracks on the concrete surface will increase the salt scaling resistance, and beside the crack width, a number of cracks proved to be an important factor influencing concrete resistance to salt scaling. Previous carbonation of RAC decreases the salt scaling resistance of concrete for more than 2.5 times. The reinforcing steel surface close to the crack started to corrode quickly, at the first day of exposure to chloride rich environment. The steel bars far from the crack (35 mm and 55 mm distances), remained in passive state in RAC with 20 mm concrete cover, even after 160 days of exposure to 3 % NaCl electrolyte*

***Key words:*** *Recycle aggregate concrete, cracks, salt scaling, carbonation, corrosion*

## 1. INTRODUCTION

Great impact of the construction industry on the environment is mainly influenced by the enormous use of raw materials, great energy consumption and large waste production. A large part of the burden lies down on concrete industry having in mind that concrete is one of the most widely used construction materials in the world. The use of river gravel and large carbon-dioxide footprint from cement production are the main problems of non-sustainable concrete production. Use of recycled concrete aggregate (RCA) for the production of new concrete can be a promising solution [1,2]. However, durability of recycled aggregate concrete (RAC) remains as an important issue regarding its sustainability.

****This manuscript is dedicated to the memory of Professor Miomir Pavlović**

*Corresponding author: Jelena Bajat[3]
E-mail: jela@tmf.bg.ac.rs
Paper received: 16.08.2026.
Paper corrected: 19.10.2026.
Paper accepted: 22.10.2026.

Therefore, due to the intensive development of RAC as a construction material, it is crucial to show that this type of concrete represents a viable alternative to natural aggregate concrete (NAC), which would lead to its greater use in practice both from mechanical and durability point of view.

With relatively low tensile strength of concrete, the cracking of structural elements is almost inevitable due to the effect of load. Cracks damage the structure of concrete cover and represent the channels for transport of harmful agents, leading to concrete deterioration and as a final result, to the corrosion of reinforcement [3–4]. Despite of this and thanks to the complexity of their influence, the cracks has not been taken yet into account as a parameter in defining the service life of concrete structures in [5].

Presence of chlorides from different sources in contact with concrete is a common occurrence in many concrete applications [6]. This may cause the deterioration of reinforced concrete structures in two different mechanisms. First, chlorides can induce the corrosion of reinforcement. Secondly, they can damage the concrete surface as a result

of freezing and thawing cycles with salt solution on the concrete surface (salt scaling).

Reinforcement corrosion is an electrochemical reaction of steel surface with oxygen in the presence of moisture at a specified temperature. The appearance of reinforcement corrosion will cause a reduction in adhesion between bars and concrete, reducing the cross section area of bars, and increasing local stresses in concrete. During the process, $Fe^{2+}$, $Cl^-$ and $H^+$ ions are still present in the cavities and pH value may fall locally to the value of 5. The process of corrosion caused by chlorides, especially in an alkaline environment, depends on the constant inflows of aggressive substances, it's propagation in existing cavities and initiation of the new ones [4].

Regarding the salt scaling, a damage caused by this process is progressive and consists of small flakes of paste (cement and supplementary cementitious material if used) with very few small aggregate parts removed. This reduces the concrete cover which is the only barrier to prevent penetration of moisture and other harmful substances to the reinforcement. Although several models for this phenomenon can be found in the literature [7,8,9], the mechanism of this damage is not yet fully explained. Recently, the glue spall mechanism was proposed as the primary cause of the salt scaling [10]. Numerical and experimental confirmation of this theoretical assumption can be found in the literature [11]. Effects of other deterioration mechanisms on concrete resistance to salt scaling are reflected in the change of concrete surface structure and some of them such as carbonation may have a beneficial effect. Crystals of calcium carbonate ($CaCO_3$) formed during the carbonation process have a higher volume compared to the starting reaction compounds. Accordingly, the carbonation of hardened cement paste in concrete makes concrete structure denser, reduces porosity and water absorption [12], [13], and thus improves the resistance of paste to salt scaling [11]. This phenomenon was tested on NAC [14] but not tested on RAC.

### *1.1. Influence of RCA on chloride ingress in RAC*

In comparison with the natural aggregate, RCA is more porous due to old cement paste, which is located on its surface. RAC actually has two types of interfacial transition zone (ITZ): old zone between the original natural aggregate and old mortar, and a new zone between old and new mortar [15], [16]. This makes the microstructure and thus, the durability of RAC, more complex.

The volume of ITZ in concrete increases with the use of RCA in the mixture, resulting in increased permeability and water absorption [17]. This leads to a negative impact on the resistance to salt scaling [18], [19]. Also, with increasing the replacement level of natural aggregate, the amount of free water on the concrete surface (bleeding) is also increasing, further reducing the surface strength and decreasing the resistance to salt scaling [19], [20]. Chloride ions (from sea water or de-icing salts) relatively quickly penetrate through hydrated cement paste and leach $Ca(OH)_2$, making the structure more porous [21]. Having in mind that RAC has two ITZ (old and new), their susceptibility to $Ca(OH)_2$ leaching increases and resistance to salt scaling decreases. Experimental results showed lower scaling resistance of RAC in relation to NAC [19], [20]. Also, leaching of $Ca(OH)_2$ leads to a reduction in the pH value.

Having in mind that RAC has higher porosity compared to the reference NAC, it has a lower resistance to chloride penetration [18], [19], [22], [23]. This results in higher chloride diffusion coefficient of RAC [18], [24]. However, some results from the literature show that the use of previously carbonated RCA may lead to the increase in the resistance to chloride penetration compared to the referent NAC [17], [25]. However, there is still lack of results regarding corrosion of embedded reinforcement bars in RAC.

### *1.2. Influence of cracks on reinforcement corrosion*

Numerous tests have been dealing with the phenomenon of reinforcement corrosion in concrete samples without cracks, and much less taken the cracks into account. The crack width is considered as the most important factor that affects the transport properties of chlorides and the beginning of reinforcement corrosion, Table 1. The term "critical crack width" in Table 1, refers to the width of which further increase affects the change of a $Cl^-$ ion diffusion coefficient. Crack widths below the limit values have no influence on chloride induced corrosion development, while wider cracks have an impact on reducing the period of initiation and propagation of corrosion reinforcement.

*Table 1. Influence of crack width on chloride induced corrosion*

| Reference | Method to produce cracks | Critical crack width [mm] |
|---|---|---|
| [27] | Expansive core method | 0.50 |
| [3] | Three point bending | 0.40 |
| [28] | Three point bending | 0.20 |
| [29] | Flexural cracks | 0.20 |
| [30] | Wedge splitting test | 0.20 (0.135)* |
| [31] | Four point bending | 0.14 |
| [4] | Four point bending | no relationship |

*reducing the diameter and signs of corrosion

Obviously, some of the defined critical widths (Table 1) are greater, and some are smaller than permitted crack widths in European standard EN1992-1-1 [26] for given exposure condition, which is 0.3 mm.

Initiation of corrosion depends on the crack width, but propagation is significantly affected by the level of damage on the contact between the concrete and reinforcement [2], [32]. Crack width will also affect the type of corrosion that will occur [33]. In the case of cracks narrower than 0.4 mm, pitting corrosion of the reinforced bar will be pronounced, while wider cracks will induce corrosion over a relatively large area [2]. Influence of different concrete types (concrete composition) on reinforcement corrosion is mainly expressed through the self-healing effect of concrete [34]. Favorable effect of cracks on concrete resistance to salt scaling was recorded [35]. However, there is not enough research on the influence of crack widths on this deterioration mechanism[36].

## 2. OBJECTIVES AND METHODOLOGY

The influence of cracks on the development of reinforcement corrosion in NAC was a topic of many studies. On the other hand, there is still a lack of results regarding the impact of the crack width on the development of corrosion in RAC. Also, experimental results of crack width influence on concrete resistance to salt scaling are still missing for both NAC and RAC. The main objectives of this study were to determine:

- The influence of loading induced cracks on the resistance to salt scaling of RAC,
- The impact of carbonation on RAC resistance to salt scaling,
- The influence of loading induced cracks on the chloride induced corrosion.

Measuring of scaled material was performed according to national standard, SRPSU.M1.055, after every 5 cycles of freezing and thawing using measuring scale. Resistance to salt scaling was defined with cumulative amount of scaled material per unit of exposed surface. This method was used for qualitative and quantitative analyses of RAC scaling resistance. In this way resistance to salt scaling of concrete with various crack widths and exposure conditions (carbonation) can be compared.

The onset and the development of corrosion process on steel reinforcing probes were monitored by three different electrochemical measurements:

- Open circuit potential ($E_{ocp}$) monitoring,
- Electrochemical impedance spectroscopy (EIS) technique,
- Linear polarization resistance (LPR).

Open circuit potential is the most widely used standard technique for assessing the corrosion state in concrete. Open circuit potential refers to the difference in electrical potential between working and reference electrode. The $E_{ocp}$ readings were taken simultaneously with other electrochemical measurements, using saturated calomel reference electrode (SCE). According to the standard ASTM C876[37], the probability that corrosion would occur is greater than 90 % if steel potentials in concrete are more negative than –0.270 V vs. SCE. In general, $E_{ocp}$ values are used to estimate the time of corrosion initiation and cannot be used for obtaining information about steel corrosion rates.

The EIS has become an important method of characterizing corrosion performance of steel in concrete [38]. In EIS experiments, a 10 to 50 mV sinusoidal voltage signal is applied to an electrode interface (a corroding electrode), and resulting current signal occurring at the same excitation frequency is measured. The voltage and current signals are related by the impedance in a form that is analogous to Ohm's law [39]:

$$Z(\omega) = V(\omega)/I(\omega) \quad (1)$$

The term $Z(\omega)$ is called the complex impedance and depends on the relationship between the amplitudes of the voltage (V) and current signals (I) as well as the phase shift between them ($\omega$). The technique is called spectroscopic because the impedance is measured over a domain of discrete frequencies. At the high-frequency end of the domain, only the electrolytic cell solution resistance is contained in the complex impedance. As the frequency is lowered, interfacial resistance at the corroding surface contributes to the complex impedance. Electrochemical and diffusion processes related to corrosion are detected at frequencies between about 10 and $10^{-6}$ Hz. However, it is rare that measurements are made below $10^{-3}$ Hz due to the instability of corroding surface.

In corrosion studies, EIS data are commonly presented in complex plane (Nyquist) plots and Bode plots. In this work only Nyquist plots are shown, so we give their brief explanation. In Nyquist diagram, the complex impedance at each frequency is located according to its real and imaginary components. Capacitive response, like that associated with steel in passive state, is represented by straight or nearly straight line along the imaginary axis. Charge transfer process, like that associated with pitting or active corrosion, is usually presented by partial or complete semicircular arc in the complex plane [39].

Third method for monitoring the corrosion initiation and propagation at steel rebars in RAC,

was by estimating the corrosion current density, $j_{corr}$, using linear polarization resistance method. Principles and fundamental knowledge of this method were presented by Broomfield [40]. A slow potential sweep rate was applied ±10 mV vs $E_{ocp}$ and the corresponding current was followed in order to determine the linear polarization resistance $R_p$ [41]. The polarization resistance, $R_p$, is determined as a slope of experimental curves (d$E$/d$j$) at $E_{ocp}$, and then converted to $I_{corr}$ with Stern-Geary equation [42]:

$$I_{corr} = B/R_p \quad (2)$$

The value of Stern-Geary coefficient B varies between 13 and 52 mV, depending on the state of corrosion (active or passive state). Values of 26 mV for active and 52 mV for the passive state of corrosion in concrete have been adopted and used by many authors [3, 4, 43-45]. However, the accurate value of B constant depends on the type of corrosion (pitting, galvanic, uniform, with or without oxygen diffusion limitation, etc.) [46]. Corrosion current density $j_{corr}$ is determined from the expression:

$$j_{corr} = I_{corr} / A \quad (3)$$

where $A$ is exposed surface of reinforcing bar. Linear polarization resistance technique was applied for a quantitative assessment of the corrosion state of steel rebar.

## 3. EXPERIMENTAL PROCEDURES

### *3.1. Materials and mix proportion*

The RAC was made with natural river sand and recycled coarse aggregate with a 16 mm maximum nominal size. Natural fine aggregate was commercially available river sand from the Danube River in Serbia. Recycled concrete aggregate was obtained from a demolished 40 year old highway bridge in the vicinity of Belgrade, Serbia. The aggregate was obtained by crushing columns and bridge deck in a construction site mobile crusher. The demolished structure was relatively clean from impurities as the asphalt had been scraped of the deck prior to demolition. After crushing, RCA was sieved into fractions II (4-8 mm) and III (8-16 mm). Sample cores taken from the existing structure prior to crushing, show a compressive strength of 23 MPa in the column and 35 MPa in the deck of the bridge.

*Table 2. Mixture proportion of RAC*

| Mix ingredients | (kg/m$^3$) |
|---|---|
| Coarse aggregate, 8–16 mm | 460.3 |
| Coarse aggregate, 4–8 mm | 552.6 |
| Fine aggregate, 0–4 mm | 817.0 |
| Cement CEM II S-L 42.5R | 285.0 |
| Total water | 175.0 |
| w/c | 0.614 |

The commercially available blended Portland cement CEM II/A-M (S-L) 42.5R was used. This type of cement has additions (grinded slag and limestone) up to 20 % of the total mass. Cement measured density is 3040 kg/m$^3$.

*Table 3. Properties of fresh and hardened concrete*

| | |
|---|---|
| Fresh concrete density [kg/m$^3$] | 2281 |
| Hardened concrete density [kg/m$^3$] | 2241 |
| Entrained air [%] | 3.2 |
| Slump [cm] | 14.8 |
| $f_{c,14}$ [MPa] | 34.0 |
| $f_{c,28}$ [MPa] | 41.6 |

The RAC was made in a manner that 100 % of natural coarse aggregate was replaced with RCA. The proportioning of the concrete mixtures was based on the absolute volume method. The concrete mixture proportions are given in Table 2. Physical and mechanical properties of RAC are shown in Table 3.

### *3.2. Casting, curing and testing of specimens*

For the compressive strength and specific concrete resistivity testing at all ages, 15cm cube concrete samples were prepared. Salt scaling resistance and chloride induced corrosion were tested on reinforced concrete 10x10x50 cm prisms. Prismatic samples had a reinforcing bar at the bottom of the sample (Figure 1). For the purposes of corrosion tests and mapping of corrosion products, in addition to the main reinforcing bar, three small pieces of reinforcement were added at different distances from the artificially induced crack. High yield, smooth, cold-rolled reinforcing bars were used, with a diameter of 12 mm (Figure 1). All samples were cast in steel moulds and concrete was compacted using a vibrating table. After finishing, the specimens were covered with wet fabric and stored in casting room at 20±2 $^o$C. They were demoulded after 24 h. After that, concrete cubes were kept in a water tank until testing and concrete prisms were covered with wet fabric for additional 7 days.

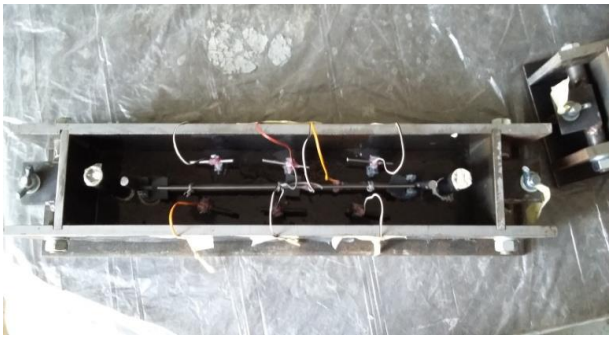


*Figure 1. Preparation of the sample for chloride induced corrosion testing*

After 28 days, three point bending was applied on prisms to induce cracks. Setup of the experiment is shown in Figure 2. Rigid steel box-profile was set on the bottom of the sample to serve as a support for the whole system. The force is applied on the concrete prism using a torque wrench and a steel cylinder which is set in the middle of span, between the concrete element and steel profile. After the crack width reached a desired dimension, applying of force using a torque wrench stopped.



*(a)* *(b)*

*Figure 2. Experiment setup: (a) for salt scaling, (b) for corrosion measurement*

Freeze and thaw tests with de-icing salt solution were performed during 25 cycles. One cycle consisted of placing the specimens in a "freezing" environment where the temperature of air is reduced to –20±2.0 °C for 16-18 h; then the specimens were moved to the laboratory and cured in air conditions at 23±3 °C for 6-8 h. This method consists of confining a pool of 3 wt% NaCl solution with a depth of 3 mm on the concrete surface. It is known that the maximum damage occurs with a moderate amount of NaCl in the solution. This "pessimum" of solute concentration occurs at 3 wt% [47]. After every 5 cycles the amount of scaled material from the concrete surface was measured. Two types of samples were prepared: cracked samples (crack width of 0.08 and 0.2 mm) and referent samples without cracks. To examine the influence of carbonation on the salt scaling resistance, samples with cracks (crack width of 0.08 and 0.2 mm) and without cracks were exposed to 2 % of carbon-dioxide ($CO_2$) for 28 days at a relative humidity of 65 % and a temperature of 20 °C. This was carried out in the carbonation chamber MEMMERTICH260C. Concrete sample labels and notation are shown in Table 4 and Figure 3.

In order to examine the influence of cracks on the reinforcement corrosion, a 0.15 mm crack was made in the middle of the concrete prism. During the chloride induced corrosion test the samples were subjected to 160 days of ponding. The electrochemical measurements were carried out at room temperature. A three-electrode arrangement was used, consisting of a stainless steel plate as a counter electrode, a SCE reference electrode, and the steel rebar as a working electrode. The reference and counter electrode were placed in a pond with NaCl solution, at the top of the concrete cover. The $E_{ocp}$ of each steel rebar was measured during the exposure of concrete prisms to 3 wt% NaCl solution.

*Table 4. Labels of the concrete samples in this study and their crack width*

| ID | Type of sample | Number of cracks | Crack pattern [crack width] |
|---|---|---|---|
| RAC_NC_0 | cube | - | - |
| RAC_C_0 | prism | - | - |
| RAC_NC_1 | prism | 2 | 0.08 / 0.03 |
| RAC_C_1 | prism | 2 | 0.08 / 0.08 |
| RAC_NC_2 | prism | 3 | 0.20/0.20 / 0.05 |
| RAC_C_2 | prism | 2 | 0.20 / 0.15 |
| RAC_NC_3 | prism | 1 | 0.15 |

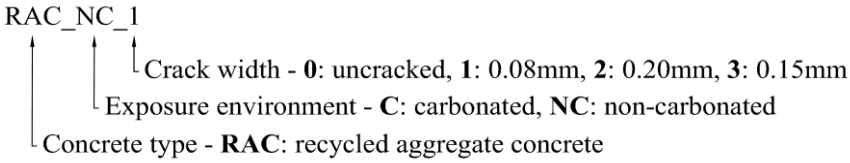



*Figure 3. Specimen notation used in the presentation of experimental results*

Electrochemical impedance spectroscopy (EIS) data were obtained at the open circuit potential using a reference 600 potentiostat/galvanostat/ZRA (Gamry Instruments), over a frequency range of 100 kHz to 10 mHz using 7 mV amplitude of sinusoidal voltage. The impedance data were fitted

to an equivalent circuit to obtain the parameters of interest in the system, by using specific software, Gamry Instruments Echem Analyst fitting program, version 5.50. The corrosion rates of the steel bars were determined using linear polarization resistance (LPR) method, polarizing samples ±10 mV vs. $E_{ocp}$, with the sweep rate of 0.1 $mVs^{-1}$.

## 4. EXPERIMENTAL RESULTS AND DISCUSSION

### *4.1. Resistance to salt scaling*

*The influence of cracks on RAC resistance to salt scaling*

Figure 4 shows a diagram of the cumulative mass of scaled material of samples with (RAC_NC_1, RAC_NC_2) and without (RAC_NC_0) cracks. The crack width of 0.08 mm (RAC_NC_1) reduced the amount of scaled material for 1.58 times compared to the sample with no cracks. Less impact on reducing the amount of scaled material was observed in the sample with crack width of 0.2 mm (RAC_NC_2). This sample had 1.11 times larger amount of scaled material compared to the sample with crack width of 0.08 mm. After 15 cycles, a mass of scaled material in RAC_NC_2 sample compared to uncracked sample was almost the same, while at the end of the test (25 cycles) quantity of scaled material was 1.42 times smaller compared to uncracked sample. Wider cracks (0.2 mm) act as an additional exposed surface thereby increasing the amount of scaled material. The value of the cumulative mass of scaled material for all three types of samples was in the range 1.98÷3.12 $kg/m^2$ which represents the expected value for this type of concrete. Values that can be found in the literature may range between 1.63÷4.34 $kg/m^2$[25].

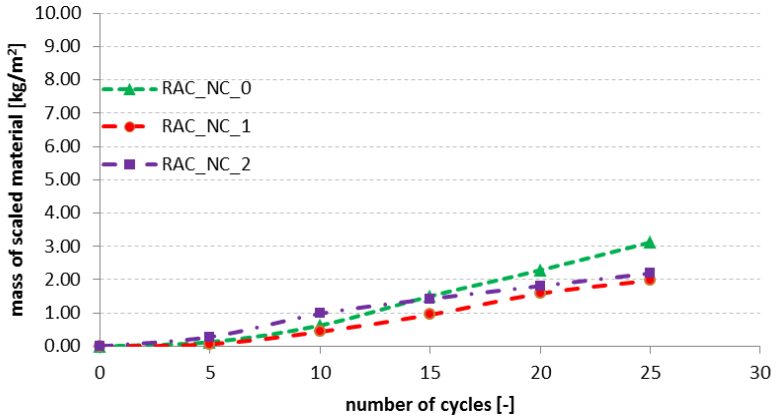



*Figure 4. Influence of crack widths on mass of scaled material: non-carbonated samples*

A similar phenomenon of crack influence was observed with carbonated samples. The values of the cumulative amount of scaled material on carbonated samples with (RAC_C_1, RAC_C_2) and without cracks (RAC_C_0) are shown in Figure 5. Occurrence of cracks of a smaller width of 0.08 mm (RAC_C_1) reduced the amount of scaled material for 1.51 times in comparison to the uncracked samples (RAC_C_0). Samples with cracks of a greater width, i.e of 0.2 mm (RAC_C_2), showed less resistance compared with samples with a crack width of 0.08 mm and almost the same resistance compared to uncracked samples after 25 cycles of freezing and thawing with de-icing salt. However, there is a difference between carbonated and non-carbonated samples with 0.2 mm cracks. Namely, regardless of the wider cracks and therefore a larger exposed surface, sample RAC_NC_2 has a smaller amount of scaled material compared to uncracked samples. This is not the case with RAC_C_2 sample. Besides carbonation, there is another difference between the RAC_NC_2 and RAC_C_2 sample. While the former has three cracks, the latter has only two cracks (Table 4 and Figure 6).

To understand the influence of cracks on the salt scaling, it is primarily necessary to understand the mechanism of damage in salt scaling. As previously pointed, when water freezes on the concrete surface it forms a composite of two materials (ice and concrete). As the composite temperature is reduced below the melting point of the solution, the ice layer tends to contract 5 times as much as the underlying concrete, which will lead to the formation of tensile stress in the ice [8]. Cracks in ice will also propagate through the cement matrix. The pressure of crystals in the open pores in the concrete crack will form a small damage that will propagate into a plain parallel to the concrete surface. This will result in the removal of a scallop [10].

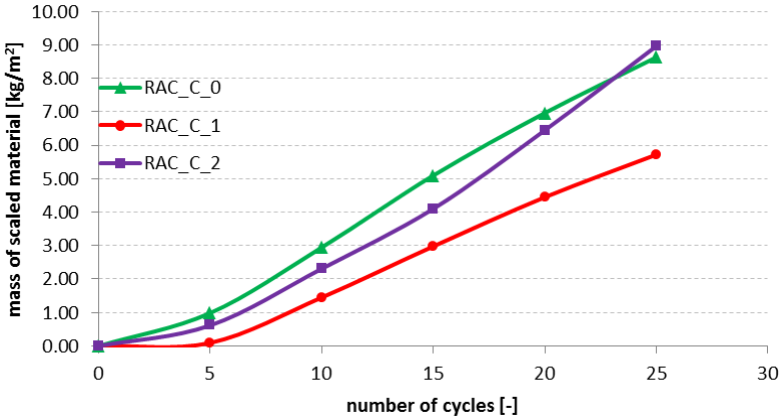
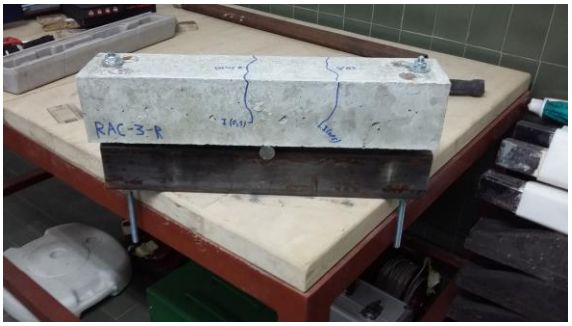
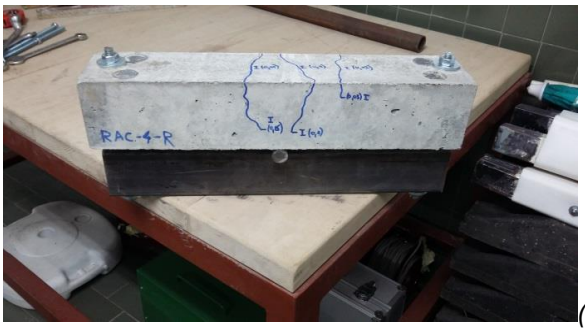



*Figure 5. Influence of crack widths on mass of scaled material: carbonated samples*

If there are cracks on concrete surface ("expansion joint") there will be a relaxation of the tensile stress in the ice, so the amount of scaled material will be smaller. Relaxation of that stress will depend on the number and spacing between "expansion joints". Accordingly, the appearance of cracks will cause a reduction of tensile stress in the ice and reduce the amount of scaled material. So, the difference in resistance between the samples with 0.2 mm cracks was due to the number of cracks which were formed on the sample surface (Figure 6). Sample RAC_NC_2 had 3 cracks (0.25, 0.20 and 0.05 mm), while the sample RAC_C_2 had only 2 cracks (0.20 and 0.15 mm). Therefore, RAC_NC_2 sample had a greater number of "expansion joints" in the process of ice shrinking, which reduced the amount of scaled material compared to uncracked sample RAC_NC_0. On the other hand, RAC_C_2 sample had a smaller number of "expansion joints" and their favorable influence has not come to expression in contrast to the negative impact of additional exposed surface.




*(a)*




*(b)*

*Figure 6. Position of cracks on samples (a) RAC_NC_2 and (b) RAC_C_2*

*Influence of carbonation on concrete resistance to salt scaling*

Cumulative amounts of scaled material for carbonated and non-carbonated samples of concrete made with recycled aggregates are shown in Figure 4 and Figure 5. Although there is an opinion that carbonation of hardened cement paste in concrete makes concrete structure denser, our tests showed that carbonation of both cracked and uncracked RAC samples, regardless of the crack widths, increased the amount of scaled material. For example, if the uncracked samples are compared, the scaled mass is 2.77 times higher for RAC_C_0 as compared to non-carbonated sample RAC_NC_0. This difference was noticeable from the start of the testing. The cause may be the fact that the carbonation makes the old ITZ and hardened cement paste brittle [13], which affects their resistance to salt scaling. Our results have shown that use of coarse recycled aggregates can decrease salt scaling resistance if the concrete surface was carbonated before the testing, which is contrary to the opinion that can be found in other literature [11].

### *4.2. The influence of cracks on chloride induced corrosion*

*Electrochemical impedance spectroscopy (EIS)*

As already pointed, onset and the development of corrosion process on steel reinforcing probes in

the sample RAC_NC_3 were monitored by electrochemical measurements.

The sample contained four steel rebars (Figure 7). In order to estimate crack influence on the overall rebar corrosion, a long steel probe (FeV2) was embedded in prism. Three small rebar probes were embedded in concrete prism at different distances from loading induced crack, as well (Figure 7). One small rebar probe (Fe6) was placed in the middle of the sample (position below the crack) while the other two were placed at 35 mm (Fe4) and 50 mm (Fe5) from the crack. The aim was to perform the corrosion mapping and to examine the effect of longitudinal micro cracks that occur around the main crack. It was found by others that the larger the crack width, the longer is the de-bond region, which potentially has an important impact on reinforcement corrosion [48].

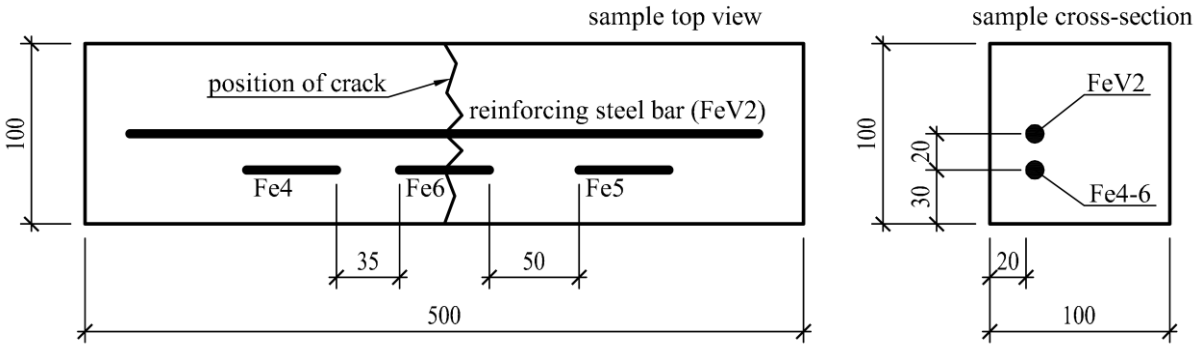



*Figure 7. Positions of the working electrodes in the concrete*

The $E_{ocp}$ evolution of each steel rebar in RAC during the 160 day exposure of concrete prisms to 3 % NaCl solution is shown in Figure 8. The comparison of the recorded $E_{ocp}$ values with the data presented in ASTM C876[37] shows interesting features. Figure 8 shows that, after small initial potential decay, Fe4 and Fe5 probes remained passive during more than 160 days, since their $E_{ocp}$ was not below –0.250 V. On the contrary, the Fe6 probe, placed below the crack, and the long steel rebar, FeV2 probe, were active already after one day of exposure to NaCl. It should be noted that Fe6 probe showed potentials of between –0.60 and –0.70 V, which is a potential of steel immersed in 3 % NaCl solution, suggesting active attack on this sample. On the other hand, the potential plateau of ~ –0.46 V for FeV2 was maintained throughout all exposure time. It was about 0.2 V more positive than Fe6$E_{ocp}$, and ~ 0.3 V negative as compared to Fe4 and Fe5 probes, and such $E_{ocp}$ value indicated localized attack of this probe.

In other words, the potential values of FeV2 probe were between the values of active Fe6 and passive Fe4 and Fe5rebars, suggesting that corrosion of FeV2 rebar was locally initiated, in the position below the crack, and that parts of FeV2 away from the crack were still in a passive state. So, the measured $E_{ocp}$ of FeV2 was actually a mixed potential established between passive and active parts of this steel rebar.

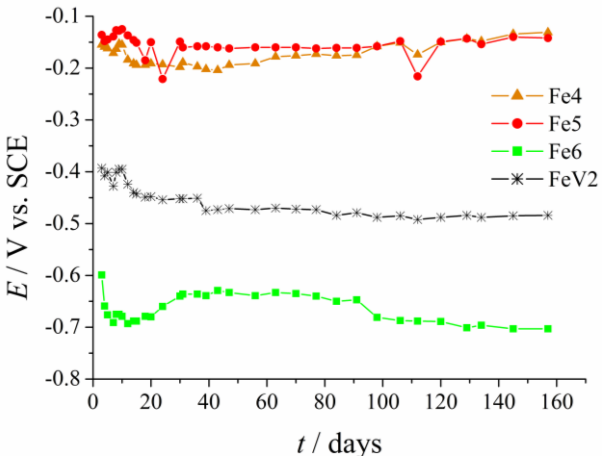



*Figure 8. The time evolution of open circuit potential, $E_{ocp}$, of steel probes inserted in RAC during exposure to 3 % NaCl solution*

The rebar probes were analyzed at certain time intervals by electrochemical impedance spectroscopy, and the Nyquist plots for the rebars embedded in RAC are shown in Figure 9. Ideally, these plots should consist of one or more semicircles, each one being a characteristic of a single "time constant". In practice, however, only a portion of one or more semicircles could be seen. The asymptotic limits of the semicircles in real part could be determined at high frequencies and at low frequencies (as the sum of all semicircle diameters,

related to the sum of all resistances that appear in the measured system). In the case where the electrode reactions occur fast i.e. the charge transfer resistance is low, an ideal semicircle could be observed. This may be marked as a resistive behavior, and denotes that corrosion process occurs on a steel rebar. After the complex impedance plots are recorded, the parameters which define the corrosion process (polarization resistance, corrosion product resistance etc.) are extracted by introducing electrical equivalent circuit which simulates the corroding interface.

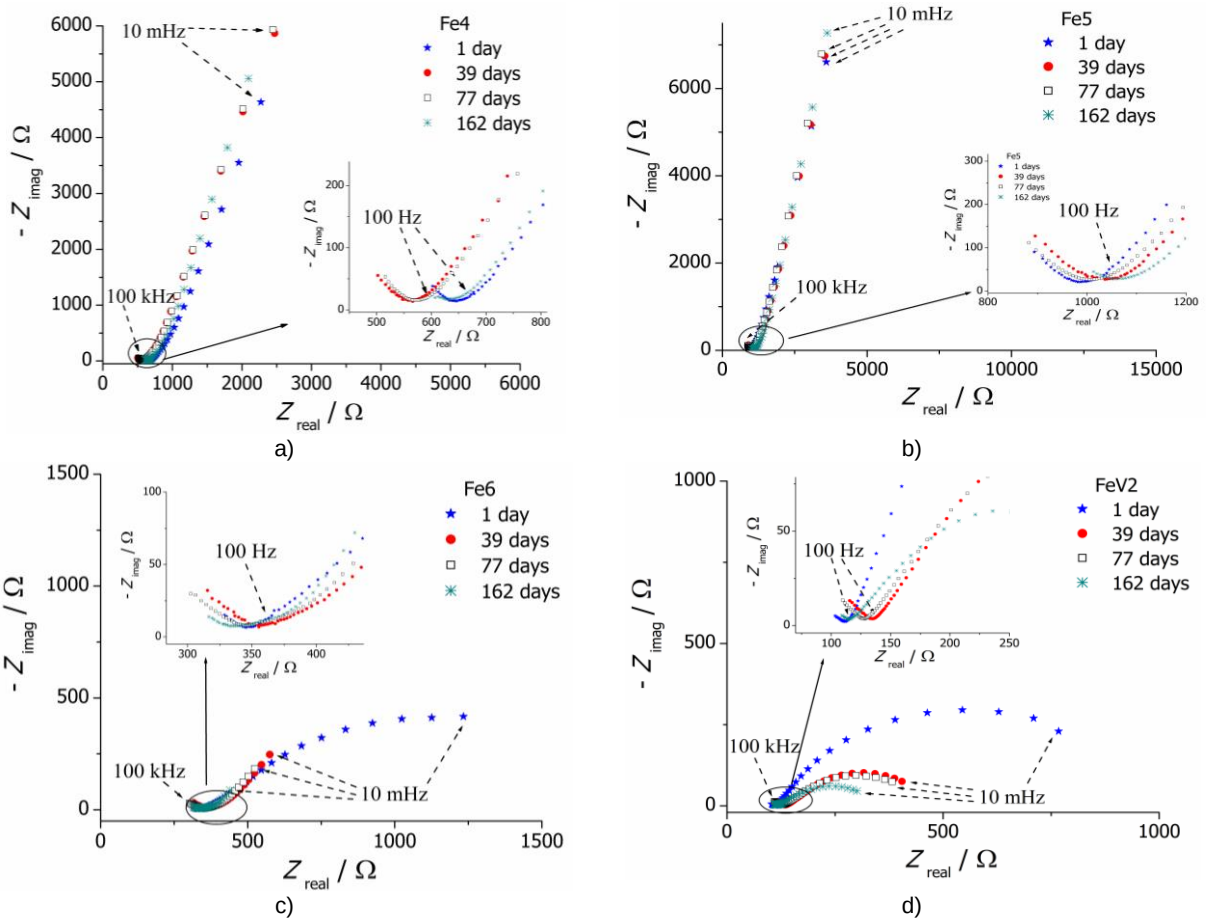



*Figure 9. The Nyquist plots for steel probes (a) Fe4 (b) Fe5 (c) Fe6 and (d) FeV2 inserted in RAC at different exposure times to 3 % NaCl solution*

Three time constants could be seen in all EIS diagrams, but the time constants at high and intermediate frequencies are better seen in insets of Figure 9. Both steel probes that were away from the crack, Fe4 and Fe5, showed capacitive response throughout all exposure time to NaCl solution, i.e. the plots consisted of a straight line almost parallel to the imaginary axis (Figure 9a and b). Their EIS data seem to overlap for more than 160 days, with the only observable change arising from the concrete properties over the time. Significantly smaller impedance values in NaCl were determined for Fe6 and FeV2rebars (Figure 9c and d). For these probes one may observe a resistive behavior, denoted by a semicircle approaching the x-axis, and with a finite radius.

The impedance spectra measured, were successfully fitted to the circuit depicted in Figure 10 using the procedure explained in previous sections. This circuit model enabled high correlation between the experimental and fitting data, and it was previously used to simulate the reinforcing steel corrosion in concrete [49].

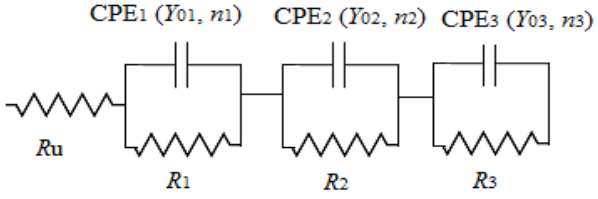



*Figure10. Equivalent electrical circuit used in the fitting process of the impedance plots*

The capacitive elements in the circuit are presented as constant phase elements CPE, quantified by $Y_o$ and n parameters. The $R_u$ element reflects the electrolyte resistance in the pond. The first time constant at high frequencies is attributed to the ionic resistance of the electrolyte in the pores of the concrete cover. The second time constant, at frequencies ~ 100Hz, was small and in some cases overlapped with the time constant in low frequency range. It may be observed only in the insets of Figure 9, and it was attributed to the ionic resistance of the film of corrosion products formed on the steel surface [49]. Finally, the third time constant in the low frequency range is linked to the surface electrochemical reactions, resulting from the contact of the rebar and corrosive agents [49].

The results obtained from the fitting procedure are shown in Table 5. The resistances related to the concrete cover ($R_1$) showed a tendency to only slightly decrease over time. On the one side, the concrete conductivity may increase as a consequence of the penetration of water molecules and chloride ions, but on the other, due to the chloride-cement reactions and the decrease in concrete porosity, the concrete resistance may increase during the exposure time [50].

*Table 5. The fitting parameters of EIS plots for rebar probes in RAC during exposure to 3 % NaCl*

| Sample ID | Time [Days] | $R_u$ [Ω] | $R_1$ kΩcm$^2$ | $CPE_1$ | | $R_2$ kΩcm$^2$ | $CPE_2$ | | $R_3$ [$10^{-4}$ Ωcm$^2$] | $CPE_3$ | |
|---|---|---|---|---|---|---|---|---|---|---|---|
| | | | | $Y_o$ [$10^8$ $s^n\Omega^{-1}$ cm$^{-2}$] | n | | $Y_o$ [$10^4$ $s^n\Omega^{-1}$ cm$^{-2}$ | n | | $Y_o$ [$10^4$ $s^n\Omega^{-1}$ cm$^{-2}$] | n |
| Fe4 | 1 | 24 | 6.06 | 3.25 | 0.47 | 8.80 | 3.31 | 0.39 | 820 | 1.75 | 0.85 |
| | 39 | 41 | 5.05 | 3.09 | 0.52 | 9.57 | 2.82 | 0.37 | 90.3 | 1.97 | 0.88 |
| | 77 | 52 | 5.58 | 4.42 | 0.48 | 4.06 | 2.42 | 0.41 | 117 | 1.92 | 0.88 |
| | 162 | 60 | 5.55 | 5.11 | 0.48 | 10.8 | 2.63 | 0.36 | 173 | 1.86 | 0.90 |
| Fe5 | 1 | 36 | 9.33 | 2.63 | 0.48 | 35.3 | 2.57 | 0.37 | 2303 | 1.51 | 0.82 |
| | 39 | 70 | 9.32 | 2.19 | 0.52 | 23.4 | 2.30 | 0.34 | 1955 | 1.52 | 0.83 |
| | 77 | 61 | 9.11 | 2.39 | 0.51 | 18.0 | 2.20 | 0.33 | 699 | 1.51 | 0.84 |
| | 162 | 52 | 5.65 | 5.11 | 0.48 | 13.4 | 2.60 | 0.36 | 190 | 1.84 | 0.90 |
| Fe6 | 1 | 38 | 3.10 | 5.15 | 0.46 | 3.29 | 4.36 | 0.34 | 1.16 | 5.04 | 0.74 |
| | 39 | 108 | 2.40 | 5.96 | 0.55 | 4.14 | 8.36 | 0.25 | 2.84 | 39.9 | 0.80 |
| | 77 | 56 | 2.82 | 7.91 | 0.51 | 1.86 | 7.45 | 0.26 | 2.19 | 77.8 | 0.75 |
| | 162 | 61 | 2.67 | 15.3 | 0.47 | 1.08 | 8.06 | 0.27 | 2.04 | 71.4 | 0.71 |
| FeV2 | 1 | 18 | 13.3 | 0.95 | 0.49 | 10.8 | 1.71 | 0.25 | 11.8 | 0.35 | 0.80 |
| | 39 | 16 | 17.2 | 2.02 | 0.48 | 8.99 | 0.82 | 0.39 | 4.14 | 0.73 | 0.74 |
| | 77 | 14 | 16.5 | 2.42 | 0.48 | 10.2 | 0.80 | 0.39 | 3.84 | 0.82 | 0.73 |
| | 162 | 16 | 14.4 | 5.79 | 0.42 | 10.3 | 0.94 | 0.38 | 2.53 | 0.97 | 0.67 |

As expected, the values of $R_1$, related to the resistance of the concrete cover, are the smallest for Fe6 rebar. This probe is right below the crack, providing a fast electrolyte ingress and correspondingly, smaller resistances. The $R_1$ resistances slowly increase with time, due to the concrete hydration. This is consistent with the measurements of concrete specific resistivity for different exposure times, where a slow, but steady, increase in the resistivity with time was shown for RAC specimens. Values of concrete specific resistance at the age of 14, 28 and 90 days, were 6.73, 7.33 and 9.17 kΩ cm respectively. The change in $R_1$ is followed with $CPE_1$ oscillations, which is interplay of greater concrete permeability due to the greater amount of water, and smaller concrete porosity due to the filling of the pores in concrete cover with hydration/corrosion products [38], [51].

The most informative data come from the change of the $R_3$ value over the exposure time, since the $R_3CPE_3$ time constant represents the corrosion reactions on the steel surface. Decrease in $R_3$ over time both for Fe4 and Fe5 probes, denotes the ingress of the electrolyte and its contact with the rebar surface, but not in a sufficient amount to destroy the protective layer on them, as can be seen from the magnitude of $R_3$ (over $10^6$ Ωcm$^2$).

The influence of the probe distance from the crack could be seen from the charge transfer resistance values, that were up to three times higher for Fe5 (55 mm away from the crack) than for Fe4 probe (35 mm away from the crack). On the contrary, and as expected from the negative $E_{ocp}$ values at all ponding times, the $R_3$ values for the probe below the crack (Fe6) were in the range between 11 and 20 kΩcm$^2$, denoting fast corrosion attack.

Nevertheless, on the basis of the shape of the EIS plots it is possible to determine whether the steel rebar is active or passive, as already

explained in part 2. Namely, the capacitive response complies with a passive rebar, while resistive one conforms to active state. In addition, Montemor [52] showed that the ratio $R_{ct}/R_s$ (related to $R_3/R_1$ in this work) could be used as an estimation of steel activity in concrete. The $R_s$ was attributed to the concrete behavior (ionic conduction of electrolyte in the concrete pores) and $R_{ct}$ is a charge transfer resistance. Passive state would be for an $R_{ct}/R_s$ ratio greater than 10, when this ratio is 5–10 there is weak steel activity, whereas values around 4 indicate intense localized attack. The criterion based on such $R_3/R_1$ ratio suggests that the Fe4 and Fe5 steel rebars were passive, while Fe6 and FeV2 active during the overall exposure period in RAC.

*Linear polarization resistance*

In order to properly estimate the corrosion type (uniform or local) of steel probes in this work, the concrete blocks were broken for visual inspection after 160 days of immersion, and the anodic areas were visually determined. As an example, Figure 11 shows the local type of attack on the long FeV2 rebar.




*Figure 11. The appearance of the long FeV2 rebar (a) in the broken concrete block and (b) enlarged after 160 days immersion*

The inspection showed corrosion products at 15 % of surface area at Fe4 and Fe5 samples, at 60 % for Fe6, and 6 % surface corroded at the long FeV2 probe. So, the sample Fe6, placed right below the crack, suffered from uniform corrosion due to its total exposure to the electrolyte ingress, the long sample FeV2 corroded locally, at positions under the crack, while the probes far from the crack suffered from localized corrosion which was in the initial phase.

The calculated $j_{corr}$ values, presented in Figure 12, show different trends for the samples at different positions in concrete. If we accept that a threshold value of $j_{corr}$, which points to the transition from passive to active corrosion, is 0.1 μAcm$^{-2}$[53], [54], it may be seen that after 18 days of ponding for Fe4 and Fe5rebars, the samples started to corrode. As Figure 12 depicts, after corrosion initiation, the $j_{corr}$ values sharply increased, then after about 50 days decreased, which was followed by $j_{corr}$ oscillations around 0.4 and 0.5 μAcm$^{-2}$. On the contrary, the Fe6 probe was corroding with quite high $j_{corr}$ values at all ponding times (high corrosion at above 1.0 μAcm$^{-2}$). As concerning the FeV2 probe, the Figure 11 clearly evidences that the local attack occurred, so in this case, the LPR method may not give the real corrosion rate [54]. Instead, a more realistic corrosion rate is obtained when the measured corrosion current density is multiplied by a factor of 10 [54], and this would bring the measured $j_{corr}$ values in localized area of FeV2 probe (Figure 12a) very close to the values of Fe6 (Figure 12b).

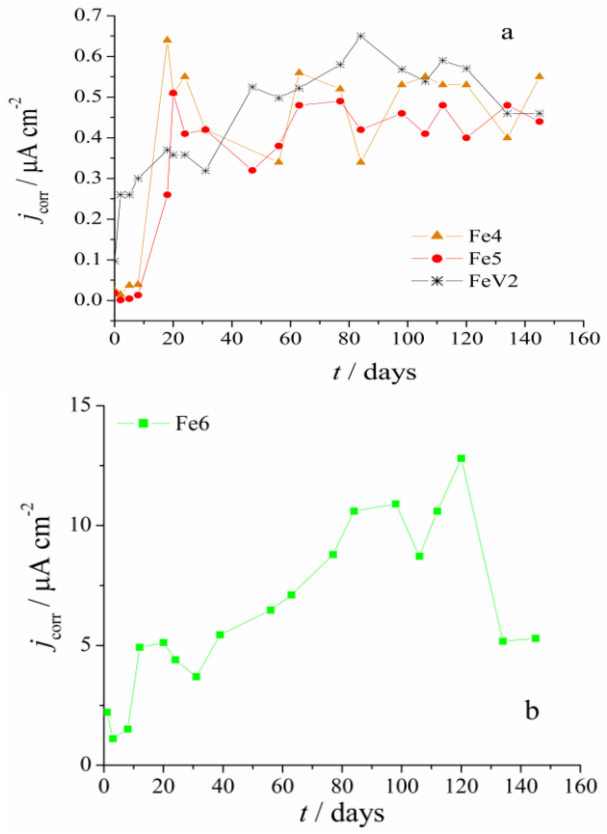



*Figure 12. The corrosion current density, $j_{corr}$, of steel probes (a) Fe4, Fe5 and FeV2, and (b) Fe6 inserted in RAC during exposure to 3 % NaCl solution*

The general conclusion on the basis of all electrochemical results is that the corrosion onset and the type of attack of steel samples embedded in RAC depend on the distance from the concrete crack. Obviously the diffusion rate of $Cl^-$ ions, as a major factor in depassivation of steel surface, was the highest right below the crack, so soon corrosion initiation of Fe6 probe occurred, and propagated as uniform corrosion. The inspection of the probes after the concrete breakage confirmed that only local, pitting attack occurred on the samples far from the crack, due to the insufficient concentration of $Cl^-$ ions. Finally, the local attack, right below the crack, occurred on the long rebar, whose behavior is important in practical applications. Such local corrosion on the long probe was predicted by $E_{ocp}$, EIS and LPR techniques. The experimentally determined $E_{ocp}$, EIS, and LPR data for FeV2 probe are actually overall responses of active and passive parts along the part of the probe which was under polarization.

Although both Fe6 and FeV2 probe corroded at the similar surface area under the crack, the calculation shows higher R values in EIS and lower $j_{corr}$ values from LPR, for FeV2 long probe. This is because the calculation considers the case when the total surface is under uniform corrosion, which was not the situation for the long sample. In addition, for long reinforcement samples the true polarized surface area during the impedance measurement is unknown [46]. So, if the fitted R values were multiplied with much lower anodic area, or with area which was under polarization, instead of the total bar surface, the calculated R values would also be lower, i.e. closer to the values for the short Fe6 probe [46].

The idea of the authors was to show that the appearance of local corrosion on a long probe, just below the crack, cannot be detected by the LPR or EIS in the initial phase. Because of this, small probes were placed to monitor the difference between uniform corrosion of a small probe Fe6 and local corrosion of a long probe FeV2 on the same place. Unfortunately, in this case corrosion is detected on the long and small probe at the same time, at the beginning of the test, so the only difference between them is higher R values in EIS and lower $j_{corr}$ values from LPR, for FeV2 long probe. In the experiment currently being conducted in our laboratory this phenomenon will be further examined.

It is accepted that the most influencing factors on the corrosion onset of steel rebars in concrete, are the presence of cracks in concrete, the concrete cover thickness, the penetrability of the cover, resistivity of concrete, and the corrosion resistance of the steel [3]. Cracks in concrete present preferential paths for the penetration of corrosion agents ($H_2O$, $O_2$, $CO_2$, $Cl^-$) [55], and this explains the loss of passivity for the sample Fe6 and the local attack of FeV2 rebar in this work, after very short period of time. However, it is important to stress out that even after 160 days, the top concrete cover of 20 mm and the distance of 35 and 55 mm from the crack, were sufficient to prevent the penetration of corrosion inducing species to the vicinity of the probes Fe4 and Fe5, respectively.

## 5. CONCLUSIONS

The following conclusions can be made from experimental results presented in this paper:

1. Presence of 0.08 mm crack width on the concrete surface will increase the salt scaling resistance of RAC.
2. Larger cracks, of 0.20 mm width, do not lead to increased resistance of concrete or further reduction of scaled material compared to smaller cracks of 0.08 mm width. Those cracks allow greater penetration of water and act like an additional exposed surface thereby increasing the amount of scaled material compared to smaller widths. In further investigation it is necessary to determine the critical crack width, which affects the improvement of salt scaling resistance of RAC concrete.
3. Number of cracks is an important factor influencing concrete resistance to salt scaling. Increasing the number of cracks (from two to three) on concrete sample leads to the relaxation of tensile stress in ice, so the amount of scaled material will be smaller.
4. Carbonation of RAC decreases the salt scaling resistance of concrete. The reason may lie in the fact that carbonation makes the old ITZ zone and the hardened cement paste brittle which decreases the salt scaling resistance.
5. The increase in the concrete resistivity with time of exposure to NaCl solution, due to the concrete hydration, was shown both by EIS and concrete specific resistance measurements.
6. The electrochemical measurements enabled mapping of corrosion initiation, propagation and corrosion rate, depending of the probe distance from the crack, during exposure to corrosion agent.
7. Namely, the steel bars far from the crack (35 mm and 55 mm distances were chosen in this work), remained in passive state in RAC with 20 mm concrete cover, even after 160 days of exposure to 3 % NaCl electrolyte.
8. On the contrary, the reinforcing steel surface close to the crack started corroding very quickly (at the first day of exposure to chloride rich

environment), due to the fast diffusion of corrosive agents through the crack. The measured $E_{ocp}$ of the long probe was a mixed potential established between passive and active parts of this steel rebar.

9. The charge-transfer resistance values for different steel probes, indicating their electrochemical activity, decreased during ponding, however at different rates, depending on the probe position relative to the crack. They were in the range between 11 and 20 kΩcm$^2$ for the probe below the crack, denoting fast corrosion attack, while they remained over $10^6$ Ωcm$^2$ for probes 35 mm and 55 mm away from the crack.
10. The visual inspection of all the probes after 160 days of exposure to NaCl solution confirmed the uniform corrosion of the rebar placed below the crack, while the probes far from the crack suffered from localized corrosion which was in the initial phase.

The appearance of cracks leads to concrete cover deterioration and to the acceleration of the transport of harmful substances through the concrete, which affects the durability of RC structures. The influence of the crack was analyzed through the test results presented in this paper. It was shown that the end of the initiation period does not necessarily mean the end of the service life.

In future research, it is necessary to examine the influence of different crack widths, primarily on corrosion of reinforcement caused by chlorides. After that, based on the analytical relationship between the reinforcement stress ratio and the crack width, a limitation of the reinforcement stress can be proposed, which would allow the entire service life (initiation and propagation period) of RC elements with cracks to meet the prescribed durability requirements.

*Acknowledgements*

This work was supported by the Ministry of Science, Technological Development and Innovation of the Republic of Serbia (Contract Nos. 200092and 451-03-34/2026-03/ 200135)

## 6. REFERENCES

[1] S. Marinković, J. Dragaš, I. Ignjatović, and N. Tošić, “Environmental assessment of green concretes for structural use,” J. Clean. Prod., vol. 154, pp. 633–649, 2017.

[2] B. J. Pease, “Influence of concrete cracking on ingress and reinforcement corrosion,” Technical University of Denmark, 2010.

[3] M. Otieno, H. Beushausen, and M. Alexander, “Chloride-induced corrosion of steel in cracked concrete - Part I: Experimental studies under accelerated and natural marine environments,” Cem. Concr. Res., vol. 79, pp. 373–385, 2016.

[4] A. Blagojevic, “The Influence of Cracks on the Durability and Service Life of Reinforced Concrete Structures in relation to Chloride - Induced Corrosio A Look from a Different Perspective,” Delft University of Technology, 2016.

[5] fib-Bulletin 34, Model Code for Service Life Design, 1st ed. Lausanne, Switzerland: International Federation for Structural Concrete (fib), 2006.

[6] P. T. Nguyen, E. Bastidas-Arteaga, O. Amiri, and C. P. El Soueidy, “An Efficient Chloride Ingress Model for Long-Term Lifetime Assessment of Reinforced Concrete Structures Under Realistic Climate and Exposure Conditions,” Int. J. Concr. Struct. Mater., vol. 11, no. 2, pp. 199–213, 2017.

[7] A. B. Harnik, U. Meier, and A. Rosw, “Combined Influence of Freezing and Delcing Salt on Concrete—Physical Aspects,” Durab. Build. Mater. Components, vol. ASTMSTP 69, p. 474–484., 1980.

[8] G. W. Scherer, “Stress from crystallization of salt,” Cem. Concr. Res., vol. 34, pp. 1613–1624, 2004.

[9] M. Yamamoto, K. Nakarai, Y. Yoshizumi, and R. Torrent, “Case Studies in Construction Materials Relationship between chloride ingress and concrete cover quality of inland structures exposed to deicing salts,” Case Stud. Constr. Mater., vol. 20, no. March, p. e03075, 2024.

[10] J. J. Valenza II and G. W. Scherer, “Mechanism for salt scaling,” J. Am. Ceram. Soc., vol. 89, no. 4, pp. 1161–1179, 2006.

[11] O. Çopuroğlu and E. Schlangen, “Modeling of frost salt scaling,” Cem. Concr. Res., vol. 38, no. 1, pp. 27–39, 2008.

[12] S. T. Pham and W. Prince, “Effects of Carbonation on the Microstructure of Cement Materials: Influence of Measuring Methods and of Types of Cement,” Int. J. Concr. Struct. Mater., vol. 8, no. 4, pp. 327–333, 2014.

[13] C. Wang, J. Xiao, G. Zhang, and L. Li, “Interfacial properties of modeled recycled aggregate concrete modified by carbonation,” Constr. Build. Mater., vol. 105, no. February, pp. 307–320, 2016.

[14] M. Leivo et al., “Effect of interacted deterioration parameters om service life of concrete structures in cold environments,” Espoo, Finland, 2011.

[15] J. Z. Xiao, B. Lei, and C. Z. Zhang, “On carbonation behavior of recycled aggregate concrete,” Sci. China Technol. Sci., vol. 55, no. 9, pp. 2609–2616, 2012.

[16] N. Otsuki, S. Miyazato, and W. Yodsudjai, “Influence of Recycled Aggregate on Interfacial Transition Zone, Strength, Chloride Penetration and Carbonation of Concrete,” J. Mater. Civ. Eng., vol. 15, no. 5, pp. 443–451, 2003.

[17] S. Yehia, K. Helal, A. Abusharkh, A. Zaher, and H. Istaitiyeh, “Strength and Durability Evaluation of Recycled Aggregate Concrete,” Int. J. Concr. Struct. Mater., vol. 9, no. 2, pp. 219–239, 2015.

[18] J. Xiao, D. Lu, and J. Ying, “Durability of Recycled Aggregate Concrete: An Overview,” J. Adv. Concr. Technol., vol. 11, no. 12, pp. 347–359, 2013.

[19] J. Andal, M. Shehata, and P. Zacarias, “Properties of concrete containing recycled concrete aggregate

of preserved quality," Constr. Build. Mater., vol. 125, pp. 842–855, 2016.

[20] Missouri Department of Transportation, "Project Title : Recycled Concrete Aggregate ( RCA ) for Infrastructure Elements Report C : Bond Behavior of Mild Reinforcing Steel in RCA Concrete" Rolla, Missouri, 2014.

[21] X. Wang, "Evaluation of de-icer deterioration of concrete," Iowa State University, Ames, Iowa, 2014.

[22] M. Gomes, J. Brito, and M. Bravo, "Structural concrete with incorporation of coarse recycled concrete and ceramic aggregates: durability performance" Mater. Struct., vol. 42, no. 5, pp. 663–675, 2009.

[23] J. Ying, J. Xiao, and Q. Meng, "On Probability Distribution of Chloride Diffusion Coefficient for Recycled Aggregate Concrete," Int. J. Concr. Struct. Mater., vol. 10, no. 1, pp. 61–73, 2016.

[24] L. F. Jimenez and E. I. Moreno, "Durability Indicators in High Absorption Recycled Aggregate Concrete," Adv. Mater. Sci. Eng., vol. 2015, p. 8, 2015.

[25] R. Movassaghi, "Durability of Reinforced Concrete Incorporating Recycled Concrete as Aggregate (RCA)," University of Waterloo, Ontari, Canada, 2006.

[26] CEN, "EN 1992-1-1," 1st ed., vol. 1, CEN, Ed. Belgrade: ISS, 2015.

[27] R. Francois, I. Khan, H. Mercado, and A. Castel, "Influence of mechanical cracks on the development of corrosion mechanism," in International RILEM Conference on Advances in Construction Materials Through Science and Engineering, 2011, pp. 578–585.

[28] A. Scott and M. G. Alexander, "The influence of binder type, cracking and cover on corrosion rates of steel in chloride-contaminated concrete," Mag. Concr. Res., vol. 59, no. 7, pp. 495–505, 2007.

[29] S. Bhaskar, R. Gettu, B. H. Bharatkumar, and M. Neelamegam, "Studies on chloride induced corrosion of reinforcement steel in cracked concrete," SDHM Struct. Durab. Heal. Monit., vol. 7, no. 4, pp. 231–251, 2011.

[30] J. Pacheco, "Corrosion of steel in cracked concrete" Delft University of Technology, Netherlands, 2015.

[31] M. Şahmaran and İ. O. Yaman, "Influence of transverse crack width on reinforcement corrosion initiation and propagation in mortar beams," Can. J. Civ. Eng., vol. 35, no. 3, pp. 236–245, 2008.

[32] G. Li, M. Boulfiza, and R. Evitts, "On the subtilities of rebar corrosion behaviour in cracked concrete," Cem. Concr. Compos., vol. 160, no. March, p. 106038, 2025.

[33] C. Martens, R. Caspeele, E. Verstrynge, C. Martens, R. Caspeele, and E. Verstrynge, "Exploring the Effects of Mechanical Cracking on the Corrosion Rate in Reinforced Concrete," in Proceedings of the CACRCS days 2025. Presented at the CACRCS days 2025, Capacity Assessment of Corroded Reinforced Concrete Structures: from research to daily engineering evaluation, 2025.

[34] C. GU, Y. Guang, and W. Sun, "A review of the chloride transport properties of cracked concrete: experiments and simulations," J. Zhejiang Univ. Sci. A, vol. 16, no. 2, pp. 81–92, 2015.

[35] Y. Cheng, Y. Zhang, Y. Jiao, and J. Yang, "Quantitative analysis of concrete property under effects of crack, freeze-thaw and carbonation," Constr. Build. Mater., vol. 129, pp. 106–115, 2016.

[36] Q. Deng, Z. Wang, S. Li, and Q. Yu, "Salt scaling resistance of pre-cracked ultra-high performance concrete with the coupling of salt freeze-thaw and wet-dry cycles," Cem. Concr. Compos., vol. 146, no. June 2023, p. 105396, 2024.

[37] ASTM, "ASTM Standard C876," in Annual Book of ASTM Standards, West Conshohocken, USA: ASTM, 2015, pp. 1–8.

[38] D. A. Koleva, J. H. W. de Wit, K. van Breugel, Z. F. Lodhi, and G. Ye, "Investigation of Corrosion and Cathodic Protection in Reinforced Concrete," J. Electrochem. Soc., vol. 154, no. 5, p. C261, 2007.

[39] R. G. Kelly, J. R. Scully, D. W. Shoesmith, and R. G. Buchheit, Electrochemical Techniques in Corrosion Science and Engineering, vol. 18. 2003.

[40] J. P. Broomfield, Corrosion of Steel in Concrete: Understanding, Investigation and Repair. London, UK: E&FN Spon, 1997.

[41] M. Otieno, H. Beushausen, and M. Alexander, "Chloride-induced corrosion of steel in cracked concrete - Part II: Corrosion rate prediction models," Cem. Concr. Res., vol. 79, pp. 386–394, 2016.

[42] M. Stern and A. L. Geary, "Electrochemical Polarization," J. Electrochem. Soc., vol. 104, no. 9, p. 559, 1957.

[43] C. Andrade and C. Alonso, "Corrosion rate monitoring in the laboratory and on-site," Constr. Build. Mater., vol. 10, no. 5 SPEC. ISS., pp. 315–328, 1996.

[44] J. A. Gonzalez, J. M. Miranda, and S. Feliu, "Considerations on reproducibility of potential and corrosion rate measurements in reinforced concrete," Corros. Sci., vol. 46, no. 10, pp. 2467–2485, 2004.

[45] S. Feliu, J. A. González, J. M. Miranda, and V. Feliu, "Possibilities and problems of in situ techniques for measuring steel corrosion rates in large reinforced concrete structures," Corros. Sci., vol. 47, no. 1, pp. 217–238, 2005.

[46] G. Song, "Theoretical analysis of the measurement of polarisation resistance in reinforced concrete," Cem. Concr. Compos., vol. 22, no. 6, pp. 407–415, 2000.

[47] J. Marchand, M. Jolin, and Y. Machabee, "Deicer salt scaling resistance of supplementary cementing material concrete: Laboratory results against field performance," in Cement Combinations for Durable Concrete: Proceedings of the International Conference, 2005, pp. 579–590.

[48] B. Savija, "Experimental and Numerical Investigation of chloride ingress in cracked concrete" Delft University of Technology, Netherland, 2014.

[49] M. Ismail and M. Ohtsu, "Corrosion rate of ordinary and high-performance concrete subjected to

chloride attack by AC impedance spectroscopy," Constr. Build. Mater., vol. 20, no. 7, pp. 458–469, 2006.

[50] B. Díaz, X. R. Nóvoa, and M. C. Pérez, "Study of the chloride diffusion in mortar: A new method of determining diffusion coefficients based on impedance measurements," Cem. Concr. Compos., vol. 28, no. 3, pp. 237–245, 2006.

[51] S. J. Ford, J. D. Shane, and T. O. Mason, "Assignment of features in impedance spectra of the cement-paste/steel system," Cem. Concr. Res., vol. 28, no. 12, pp. 1737–1751, 1998.

[52] M. F. Montemor, A. M. P. Simoes, and M. M. Salta, "Effect of fly ash on concrete reinforcement corrosion studied by EIS," Cem. Concr. Compos., vol. 22, no. 3, pp. 175–185, 2000.

[53] J. P. Broomfield, Uhlig ' S Corrosion Handbook, Third. Hoboken, New Jersey: John Wiley and sons, inc., 2011.

[54] C. Andrade, M. C. Alonso, and J. A. Gonzalez, "An initial effort to use the corrosion rate measurment for estimating rebar durability," in Corrosion rates of steel in concrete, ASTM STP 1065, N. S. Berke, V. Chaker, and D. Whitning, Eds. Philadelphia, USA: ASTM, 1990, pp. 29–37.

[55] P. Locoge, M. Massat, J. P. Olliver, and C. Richet, "Ion Diffusion in microcracked concrete," Cem. Concr. Res., vol. 22, pp. 431–438, 1992.

[56] X. Wang, M. Ba, B. Yi, J. Liu (2024) Experimental and numerical investigation on the effect of cracks on chloride diffusion and steel corrosion in concrete, Journal of Building Engineering, 86, 108521-108546. https://doi.org/10.1016/j.jobe.2024.108521

## IZVOD

### UTICAJ PRSLINA NA LJUŠTENJE MATERIJALA I PRODIRANJE HLORIDA U BETON SA RECIKLIRANIM AGREGATOM

*Primena betona sa recikliranim agregatom predstavlja značajan potencijal za unapređenje održivosti građevinske industrije, pre svega kroz smanjenje potrošnje prirodnih sirovina i energije, kao i smanjenja količine otpada nastalog proizvodnjom betona. Međutim, trajnost ovog materijala i dalje predstavlja jedan od ključnih izazova njegove šire primene. Zbog relativno niske zatezne čvrstoće, beton je podložan nastanku prslina usled delovanja opterećenja, što može negativno da utiče na vek trajanja betona. U ovom radu je ispitivan uticaj prslina nastalih pod dejstvom opterećenja (širine 0,08 mm i 0,20 mm), kao i prethodne karbonatizacije, na otpornost betona sa recikliranim agregatom na površinsko ljuštenje i otpadanje usled dejstva soli. Pored toga, analiziran je uticaj prisustva prslina na razvoj korozije čelične armature, sa posebnim osvrtom na prostornu raspodelu korozionih procesa u zavisnosti od udaljenosti od prsline. Početak i napredovanje procesa korozije na čeličnim armaturnim šipkama praćeni su primenom tri elektrohemijske metode: merenja potencijala otvorenog kola, spektroskopije elektrohemijske impedancije i metode linearne polarizacione otpornosti. Rezultati istraživanja su pokazali da prisustvo prslina na površini betona doprinosi povećanju otpornosti betona na ljuštenje i otpadanje usled dejstva soli, pri čemu, pored širine, značajnu ulogu ima i broj prslina. Nasupot tome, prethodna karbonatizacija dovodi do značajnog smanjenja ove otpornosti, i to za više od 2,5 puta. Pokazano je da površina čelične armature u blizini prsline počinje da korodira već tokom prvog dana izlaganja korozionoj sredini koja sadrži hloridne jone. Sa druge strane, delovi armature udaljeni 35 mm i 55 mm od prsline zadržali su pasivno stanje u betonu sa recikliranim agregatom, pri debljini zaštitnog sloja od 20 mm, čak i nakon 160 dana izlaganja elektrolitu koji sadrži 3% NaCl.*

***Ključne reči:*** *Beton sa recikliranim agregatom, prsline, ljuštenje usled dejstva soli, karbonatizacija, korozija*

*Naučni rad*
*Rad primljen 16.08.2026.*
*Rad korigovan 19.10.2026.*
*Rad prihvaćen 22.10.2026.*

*Vedran Carević* https://orcid.org/0000-0002-8887-6722
*Mihael Bučko* https://orcid.org/0000-0001-6992-8841
*Ivan Ignjatović* https://orcid.org/0000-0002-2679-0982
*Jelena Bajat* https://orcid.org/0000-0003-0742-8176

© 2026 Authors. Published by Engineering Society for Corrosion. This article is an open access article distributed under the terms and conditions of the Creative Commons Attribution 4.0 International license (https://creativecommons.org/licenses/by/4.0/